Computer Simulation of Steady Polymer Melt Spinning

DEL KENNETH GAGON* *and* MORTON M. DENN**

Department of Chemical Engineering
University of Delaware
Newark, Delaware 19711

An interactive computer simulation program has been developed for steady polymer melt spinning. The program includes inertial and air drag effects, and fluid viscoelasticity is described by the Phan-Thien and Tanner constitutive equation. Simulation results are compared with experiments by George on poly(ethylene terephthalate) (PET) at spinning speeds of 1000 and 3000 m/min, and the effect of elasticity under other spinning conditions is explored with computer experiments.

INTRODUCTION

The melt spinning process for the manufacture of textile fibers is shown schematically in *Fig. 1.* Molten polymer is extruded through a spinneret into cross-flowing air; the air is at a temperature below the solidification temperature of the polymer. The solidified polymer is taken up at a speed that is considerably above the mean extrusion velocity, resulting in drawing of the filament. The steady-state ratio of extrusion to takeup area is known as the draw ratio (D_R); to within the approximation that polymer density is independent of temperature, the draw ratio is also equal to the ratio of takeup to extrusion velocity. The solidified polymer is typically subjected to further downstream processing for property development. A single spinneret contains many jets, and the individual solidified filaments are taken up together to form a yarn.

The stress at solidification, equivalent to optical birefringence for a noncrystalline polymer like poly(ethylene terephthalate) (PET), is the property of the as-spun filament that is most likely to affect such ultimate physical properties of the yarn as solid modulus, extension-to-break, and dye acceptance. Commercial melt spinning is typically carried out at takeup speeds in the range 1000 to 4000 m/min, with draw ratios of several hundred. Under these conditions, the stress at solidification will be determined by interactions between fluid rheology, heat transfer, and aerodynamics. Because of the complexity of the individual phenomena and of the interactions, a process simulation is a useful tool for exploring the effect of changes in operating variables (extrusion temperature, air velocity, takeup speed, etc.) and polymer melt properties on the properties of the spun filament.

An overall picture of the extent of understanding of the various physical processes in melt spinning is contained in the book by Ziabicki (1), and the effect of viscoelasticity on the fluid mechanics is discussed more fully in the book by Petrie (2) and in the review chapter by Denn (3), where the recent literature is summarized. The process was first simulated in the steady state by Kase and Matsuo (4), using the assumptions that the molten polymer has the rheology of either a Newtonian or inelastic power law fluid, and that the takeup speed is sufficiently slow to ignore inertial and air drag effects. Agreement with experiment appears to be good. A simulation by Glicksman (5) using the same physical assumptions agrees well with velocity and temperature profile data for glass fibers. The first simulation of spinning that includes the effects of inertia and air drag seems to be that of Hamana, *et al.* (6). Similar simulations have been reported by George (7), who finds good agreement with data for the spinning of PET at 1000, 2000, and 3000 m/min, and by Yasuda and coworkers (8,9), who find

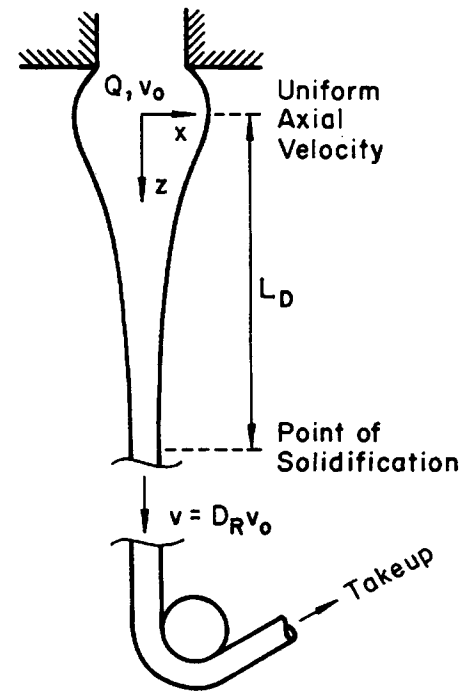

Fig. 1. Schematic of the melt spinning process.

* Present address: E. I. DuPont de Nemours and Co., Wilmington, Delaware 19899.
** Present address: Department of Chemical Engineering, University of California, Berkeley, California 94720.

agreement with birefringence calculations to 5,000 m/min. Stehle and Bruckner (10) have included inertia and air drag in a simulation of glass fiber drawing.

Viscoelasticity has been considered in general only for slow speed spinning (11-16), although Petrie (2,17) has analyzed the effect of inertia, but not air drag, on isothermal spinning with several viscoelastic models. Only Fisher and Denn (13) have included the effect of heat transfer. The most general treatment of isothermal spinning is by Phan-Thien (16), who used a stress constitutive equation that accounts for a distribution of relaxation times, shear thinning, and stress saturation at large stretch rates. A general conclusion of all of the analyses, which is supported by limited slow speed isothermal spinning data, is that, for a specified draw ratio and processing conditions, a viscoelastic liquid will draw down more rapidly than an inelastic liquid and will require a considerably higher takeup tension. Matsui and Bogue (18) have used a viscoelastic constitutive equation to analyze slow speed nonisothermal spinning experiments, but they have used experimental velocity profiles to calculate the stress. Since they have not solved a boundary value problem and satisfied the momentum equation, interpretation is difficult.

We describe here an interactive computer simulation of steady state melt spinning of a viscoelastic liquid, including heat transfer, inertial, and air drag effects. The fluid rheology is described by Phan-Thien and Tanner's constitutive equation (16,19). The discussion here focuses on PET, for which comparison with experimental velocity data at speeds up to 3000 m/min is possible, but the simulation is applicable to any polymer for which the rheological properties are available. A listing and user's guide for the complete FORTRAN-IV program is contained in Gagon (20).

PROCESS MODEL

The spinline is described by equations which are derived by averaging the conservation and stress equations over the cross-section, and they are asymptotically valid downstream from the spinneret. There is an assumption of small curvature, which could break down near the spinneret, and shear stresses developed in the spinneret are assumed to have relaxed. The most careful derivation is given by Matovich and Pearson (21). Fisher, *et al.* (22) have studied the approach to the asymptotic equations for slow speed, isothermal spinning of a Newtonian fluid, and they find that the asymptotic equations are always valid within one jet diameter of the spinneret, with the distance from the spinneret decreasing with increasing takeup force. No comparable calculation is available for any viscoelastic fluid.

The steady-state equation of conservation of mass is

$$\rho \frac{\pi d^2}{4} v = \rho Q = constant \tag{1}$$

Here, Q is the volumetric flow rate, v is the mean velocity in the spinning direction, d is the filament diameter, and ρ is the polymer density.

The steady-state momentum equation is

$$\frac{\mathrm{d}}{\mathrm{d}z}\left(\frac{\pi d^2}{4}(\tau^{zz} - \tau^{xx})\right) = \frac{\pi d}{2}\rho_a v^2 C_f + \rho Q \frac{\mathrm{d}v}{\mathrm{d}z} - \frac{\pi d^2}{4}\rho g \tag{2}$$

z denotes the spinning direction, and x is any direction in the cross-sectional plane. τ^{zz} and τ^{xx} are the components of the extra-stress in the spinning and transverse directions, respectively. ρ_a denotes the density of air, and g the acceleration due to gravity. C_f is the air drag coefficient, which will vary with axial position. The form of the correlation for C_f by Matsui (23) is used in the simulation:

$$C_f = \beta(\eta_a/\rho_a v d)^{0.61} \tag{3}$$

η_a is the viscosity of air. A value of $\beta = 0.6$ is in the mid-range of the data summarized by Matsui, and is used as the base case here. Matsui's own data correspond to a value $\beta = 0.37$. Surface tension effects are expected to be negligible for polymer melt spinning and are not included.

The steady-state equation for conservation of energy, neglecting axial conduction and viscous dissipation, is

$$\rho c v \frac{\mathrm{d}T}{\mathrm{d}z} = \frac{4h}{d}(T - T_a) \tag{4}$$

c is the heat capacity of the filament, and T and T_a are the filament and air temperature, respectively. h is the heat transfer coefficient, which will vary with axial position. The best published correlation for h seems to be that of Kase and Matsuo (24), and it is used in the simulation:

$$\frac{hd}{k_a} = \gamma(\rho_a v d/\eta_a)^{1/3}\left[1 + 8\left(\frac{v_x}{v}\right)^2\right]^{1/6} \tag{5}$$

v_x is the velocity of cross-flow air, and k_a is the conductivity of air. Kase and Matsuo report a value of $\gamma = 0.42$, and this is taken as the base case. Other correlations for h are given by Ziabicki (1). All physical properties of air in the correlations are evaluated at T_a.

The filament is assumed to solidify at a fixed temperature, which is normally taken as the glass transition temperature, and the solid phase is assumed to be nondeformable.

CONSTITUTIVE EQUATION

The Phan-Thien and Tanner constitutive equation, in the form proposed for strong flows by Phan-Thien (16), simplifies to the following form for the flow considered here:

$$\tau^{zz} = \sum_{i=1}^{N} \tau_i^{zz} \qquad \tau^{xx} = \sum_{i=1}^{N} \tau_i^{xx} \tag{6}$$

$$K_i\tau_i^{zz} + \lambda_i\left(v\frac{\mathrm{d}\tau_i^{zz}}{\mathrm{d}z} - 2(1-\chi)\frac{\mathrm{d}v}{\mathrm{d}z}\tau_i^{zz}\right) = 2G_i\lambda_i\frac{\mathrm{d}v}{\mathrm{d}z} \tag{7}$$

$$K_i\tau_i^{xx} + \lambda_i\left(v\frac{\mathrm{d}\tau_i^{xx}}{\mathrm{d}z} + (1-\chi)\frac{\mathrm{d}v}{\mathrm{d}z}\tau_i^{xx}\right) = -G_i\lambda_i\frac{\mathrm{d}v}{\mathrm{d}z} \tag{8}$$

$$K_i = \exp\left(\epsilon(\tau_i^{zz} + 2\tau_i^{xx})/G_i\right) \quad (9)$$

Some shearing terms are neglected in the averaging over the cross-section, and the averages of products are set equal to the products of the averages. $\{\lambda_i\}$ and $\{G_i\}$ are obtained from linear viscoelastic measurements; χ is related to viscous shear thinning and is obtained from the shear viscosity function. ϵ is related to stress saturation in uniform, uniaxial extension at high extension rates; ϵ has been measured only for low density polyethylene, for which the reported value is 0.015. For $N = 1$, $\chi = \epsilon = 0$, the Phan-Thien equation reduces to the upper convected Maxwell model.

The temperature dependence of stress is contained in the parameters $\{\lambda_i\}$ and $\{G_i\}$. *Equations* 7 and 8 should also contain terms of the form $\lambda_i v \tau_i d\ln T/dz$, but these did not appear to contribute significantly to the stress development and were neglected.

The rheological data contained in the simulation Subroutine "PET" and used in the calculations reported subsequently are taken from Gregory(25), who has measured the shear viscosity and the "maximum" relaxation time as functions of temperature and intrinsic viscosity. His maximum relaxation time, defined as the reciprocal of the shear rate at which deviation from a constant viscosity is observed, agrees well for limited measurements with the relaxation time obtained from Rheogoniometer normal stress measurements; the latter is the mean relaxation time $(\Sigma\lambda_i^2 G_i/\Sigma\lambda_i G_i)$. Gregory's data are adequate for $N = 1$, although the temperature dependence must be extrapolated from 265°C to the glass transition (about 70°C). A spectrum for PET is not available, but in order to account for the effect of a relaxation time distribution in the simulations that follow, the spectrum was taken to be a discrete approximation to a wedge:

$$G_i = \bar{\lambda}\,\bar{G}/N\lambda_i \quad (10)$$

$\bar{\lambda}$ and $\bar{G}$ are the mean values of relaxation time and shear modulus, respectively. The shear viscosity equals the product $\bar{\lambda}\ \bar{G}$. Gregory's maximum relaxation time is used for $\bar{\lambda}$, and $\bar{G}$ is computed from $\bar{\lambda}$ and his viscosity data. $\bar{G}$ is independent of temperature. In the absence of more complete information for PET, N was taken to be 2, with $\lambda_2/\lambda_1 = 5$. χ is taken to be zero because of the absence of shear thinning, and ϵ is set equal to 0.015.

BOUNDARY CONDITIONS

The temperature and diameter at the beginning of the spinline must be specified, together with the takeup speed and the draw ratio; the latter specify the initial velocity. The spinneret temperature suffices as the initial condition, and the spinneret diameter can be used in the absence of information about extrudate swell. The calculations of Fisher, *et al.* (22) indicate that the spinneret diameter will generally be a more satisfactory selection than the free jet swell diameter.

Initial conditions on the extra-stress are also required for the viscoelastic fluid. There are 2N stress components: $\{\tau_i^{xx}\}$, $\{\tau_i^{zz}\}$, $i = 1,2,\ldots,N$. $2N - 1$ stress conditions must be provided; fixing the draw ratio precludes specifying all $2N$ components, which would then fix the total force. Both force and draw ratio cannot be independently specified. It therefore suffices to provide the initial values of the ratios τ_i^{xx}/τ_i^{zz} and τ_i^{zz}/τ_N^{zz}, $i = 1,2,\ldots,N$. For the case $N = 1$, only the ratios τ^{xx}/τ^{zz} need be specified. This ratio has a value of $-\frac{1}{2}$ for the Newtonian fluid limit at every point along the spinline.

The ratio τ^{xx}/τ^{zz} must always be less than unity, for otherwise the force would be negative; it is likely that the same restriction applies to each component ratio τ_i^{xx}/τ_i^{zz} for $N > 1$. All solutions for extensional flows of viscoelastic fluids indicate that the ratio of transverse to axial extra-stress becomes smaller in magnitude at long time than for a Newtonian fluid; the implication is $\tau_i^{xx}/\tau_i^{zz} > -\frac{1}{2}$. Two special cases for the upper-convected Maxwell model, with $N = 1$, are of particular interest. In the high force limit of low speed, isothermal spinning, Denn, *et al.* (11) found that the ratio τ^{xx}/τ^{zz} is of order $(v/v_o)^3$ irrespective of the initial ratio (of order unity), so that the transverse extra-stress is negligible by the time that the velocity has increased threefold over the spinneret value; this represents a small portion of the spinline for large draw ratios. Denn, *et al.* also found that computed results were insensitive to the initial stress ratio as long as τ^{xx}/τ^{zz} was not taken close to unity; there was little difference in results for $-\frac{1}{2} \le \tau^{xx}/\tau^{zz} \le \frac{1}{2}$. A similar conclusion was reached in preliminary numerical experiments in this work.

Petrie (2, 17), following Matsui and Bogue (18), considered a motion in which fully-developed shear flow is followed instantaneously by uniform, uniaxial stretching at a constant rate. He showed that the transverse normal stress changes instantaneously from the zero value to the shear modulus, and then decays to its asymptotic value more rapidly than the shear stress. Thus, consistency with the neglect of shearing stresses in spinning suggests using the asymptotic value of the normal stresses in this motion. Petrie's result fixes $-\frac{1}{2} \le \tau^{xx}/\tau^{zz} < 0$, with the ratio approaching zero for large stretch rates. Based on these several asymptotic results, the initial ratio τ_i^{xx}/τ_i^{zz} is set to zero in the simulation program.

In the wedge spectrum, the component viscosities $\lambda_i G_i$ are all equal. In that case, for fully-developed shear flow, the axial stresses are in the ratio $\tau_i^{zz}/\tau_N^{zz} = \lambda_i/\lambda_N$. This ratio is retained for the initial values in the simulation program. (Petrie (2) notes that the expected approach to a linear velocity profile in the large force, low speed, isothermal limit may require $\tau_i^{zz}/\tau_N^{zz} = 0$, $i \neq N$. In either case, the largest relaxation time predominates.)

NUMERICAL SOLUTION

The differential equations are solved using a fourth order Runge-Kutta method. The initial force is estimated by the user; the distance to solidification is estimated by the analytical solution in Fisher and Denn (13), taking advantage of the weak dependence of the temperature profile on kinematics. Small increments in these values are then made, and subsequent corrections are made iteratively by linear extrapolation based on

previous values and the error in temperature and draw ratio at the assumed solidification point.

The equations become "stiff" for small relaxation times, and the simulation program will not run in the viscoelastic mode for PET with relaxation times less than 3×10^{-4} s. This is not a severe restriction in practice. The Newtonian limit, corresponding to a zero relaxation time and infinite modulus, is treated separately in the computer program.

MODEL VALIDATION

The model was run to simulate the experiments reported by George (7) on PET. The spinning conditions are shown in *Table 1*. Following George (7), the solidification temperature was taken to be 70°C, and the initial filament diameter was taken to be 0.36 mm; the latter is based on George's estimate of 100 percent area increase on extrusion. There are no other adjustable parameters.

The measured velocity profiles are shown with the simulation results in *Fig. 2* for takeup speeds of 1000 and 3000 m/min. Agreement with the high speed data is good. Failure to follow the curvature of the data near solidification is probably related to the inapplicability of the simple viscosity-temperature relation near the glass transition. Kase and Matsuo (24) include a term in the viscosity that becomes unbounded for $T \rightarrow T_g$, for example, resulting in a smooth approach to a zero velocity gradient at solidification. Agreement with the low speed data is less satisfactory, although the point of solidification is predicted accurately. In this case the calculated rate of drawdown is too slow.

The calculations in *Fig. 2* include a comparison between the use of a single mean relaxation time ($N = 1$) and two relaxation times. The difference is small, but the effect of a distribution and a longer maximum relaxation time is to move the calculated profile closer to the data for 1000 m/min. It is likely that a more complete representation of the relaxation spectrum would result in closer agreement between the simulation and experiments. It is to be emphasized again that this calculation contains no adjustable parameters, and uses the best literature values for the necessary functions and properties. On this basis, agreement between the simulation and experiment must be considered quite good. The sensitivity of the calculation to changes in parameters is considered subsequently.

The stress growth along the filament is shown in *Fig. 3*. The larger maximum relaxation time causes a slightly faster initial growth for $N = 2$, but the computed stress at solidification is essentially the same for $N = 1$ and $N = 2$. The factor-of-three increase in takeup speed results in a seven-fold increase in computed stress at solidification.

Table 1. Conditions for Spinning Experiments of George (7)

Polymer I. V.	0.67
Extrusion temperature	295°C
Air temperature	30°C
Air velocity	0.2 m/s
Spinneret hole diameter	0.25 mm
Throughput	1.75×10^{-5} kg/s
Spinneret mean velocity	18.2 m/min

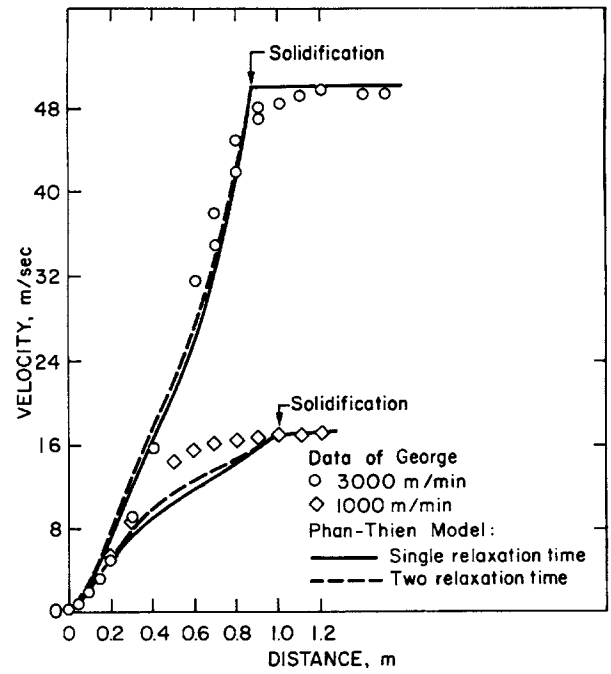

Fig. 2. Simulation of the spinning conditions in Table 1, with data of George.

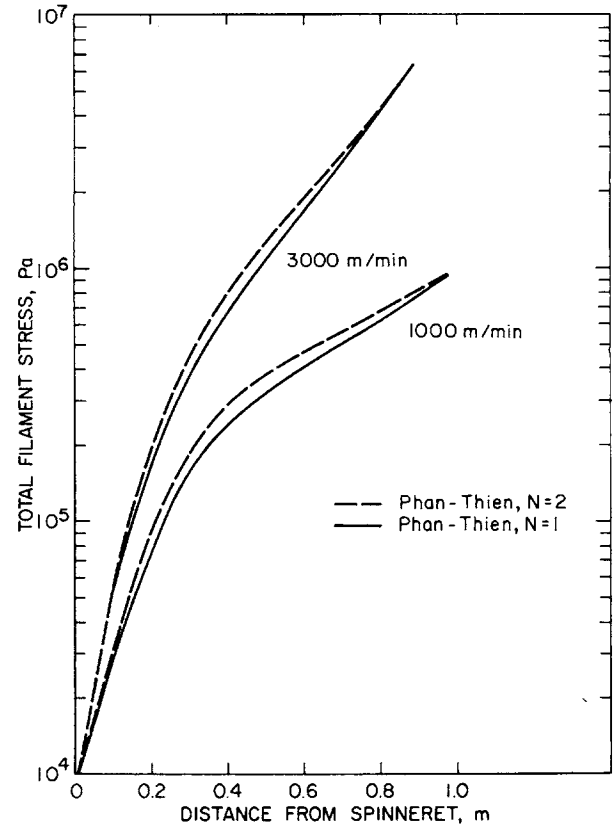

Fig. 3. Computed stress growth for spinning conditions in Table 1.

The computed temperature profiles are shown in *Fig. 4*. The location of the freeze point is relatively insensitive to the change in takeup speed. According to the approximate analytical temperature profile given by Fisher and Denn (13) and used as the first approximation, the profile would be the same for these two cases.

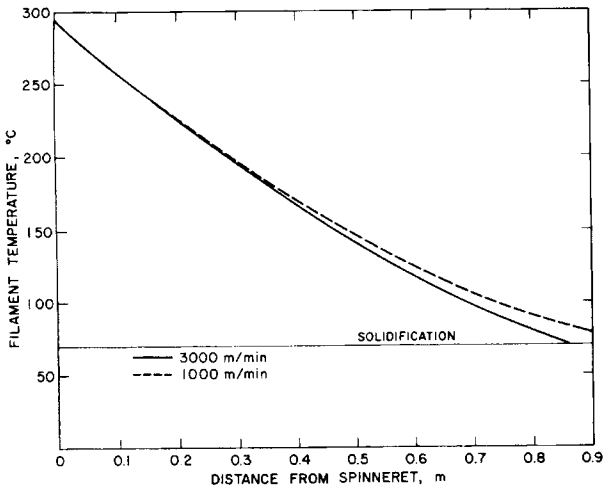

Fig. 4. Computed temperature profiles for spinning conditions in Table 1.

PARAMETRIC SENSITIVITY

Heat Transfer

We examine here the model sensitivity to some of the physical parameters. *Figure 5* shows a simulation of George's spinning data using the Newtonian fluid model. Drawdown and solidification are both too rapid at 3000 m/min relative to the data. The lines reported by George are from a simulation of the same experiments using a Newtonian fluid model (7). George may have used different correlations or constants, and his simulation is in better agreement with the data.

The dashed line in *Fig. 5* is a calculation with the simulation program developed here, assuming a Newtonian fluid, but taking the heat transfer coefficient to be only 75 percent of that given by the Kase-Matsuo correlation. This variation is within the bounds of most heat transfer correlations. Agreement with the data, and with George's simulation, is quite good. The effect of reducing the heat transfer coefficient to 75 percent of the value given by the Kase-Matsuo correlation is shown in *Fig. 6* for the viscoelastic fluid. The change is large, as would be expected. Using the available rheological data for PET, the Kase-Matsuo correlation appears to be appropriate.

The viscoelastic fluid calculation using the Kase-Matsuo heat transfer coefficient, and the Newtonian fluid calculation using the reduced heat transfer coefficient, are shown together in *Fig. 7*. On the basis of this calculation alone, given the uncertainties in both heat transfer and rheological measurement, it would not be possible to choose between the two simulations. The independent knowledge that PET is slightly viscoelastic

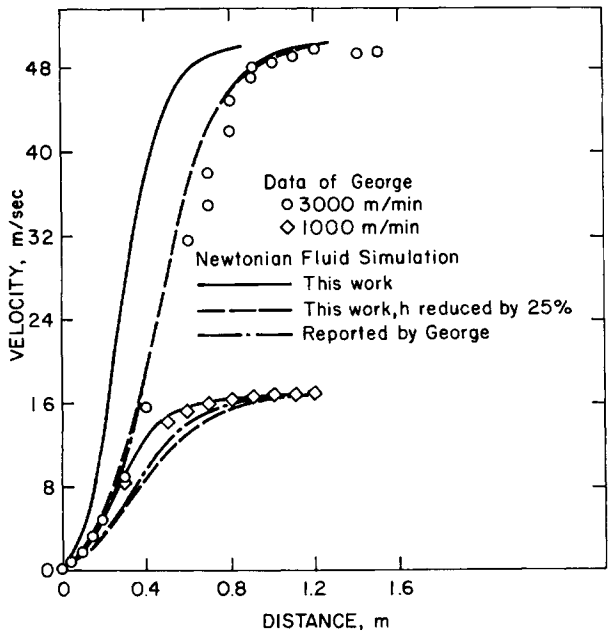

Fig. 5. Simulation of spinning conditions in Table 1, with data of George, using a Newtonian fluid model and varying the heat transfer coefficient.

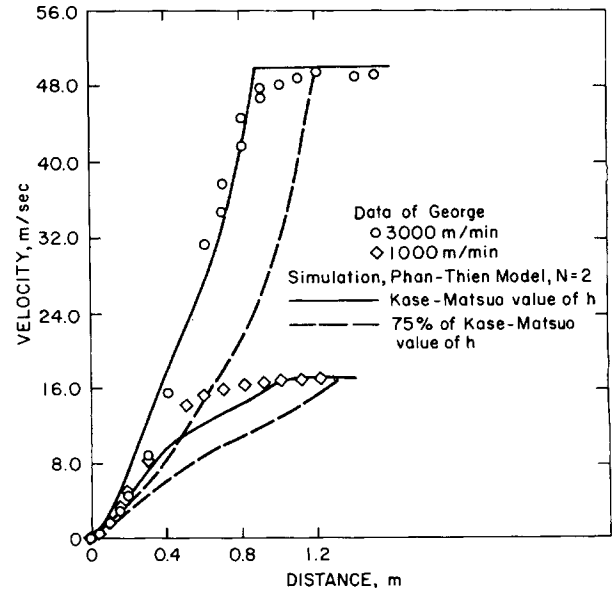

Fig. 6. Sensitivity of the simulation of the conditions in Table 1 to a change in the heat transfer coefficient.

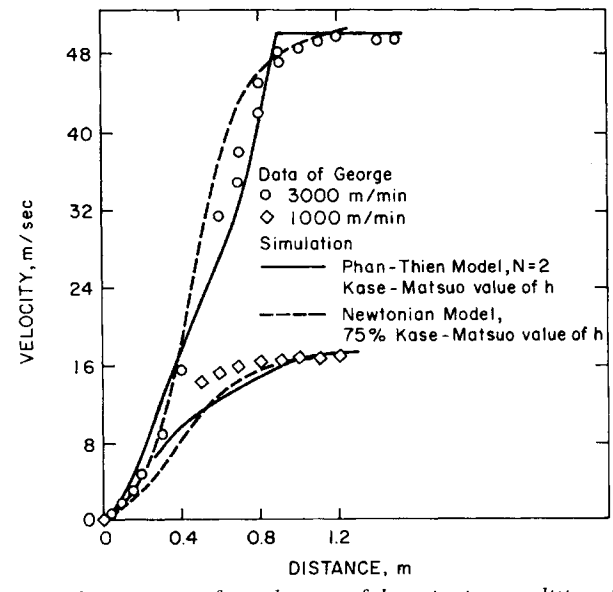

Fig. 7. Comparison of simulations of the spinning conditions in Table 1, with the data of George, using a viscoelastic fluid model and a Newtonian fluid model with a reduced heat transfer coefficient.

makes the viscoelastic fluid simulation preferable, however, and the viscoelastic fluid model should be used for extrapolation outside the range of these experiments.

Drag Coefficient

Matsui's data (23) correspond to a value of $\beta = 0.37$ in the drag coefficient correlation in *Eq 3*, rather than the value 0.6 used as the base case. The calculations in *Figs. 3* and *7* are repeated in *Figs. 8* and *9*, respectively, with the lower drag coefficient. There is a small effect, and the lower value is perhaps in better agreement with the experimental data. The sensitivity is less than that to variations in the heat transfer coefficient, however.

Rheological Parameters

The only rheological parameter in the Phan-Thien equation that is not measurable in a steady or unsteady shearing experiment is ϵ, the parameter causing stress saturation at large extension rates. Phan-Thien (16) reports $\epsilon = 0.015$ for low density polyethylene, but values have not been obtained for PET. The sensitivity of the simulation to ϵ is shown in *Fig. 10*. For these spinning conditions, there is little difference between $\epsilon = 0$ and $\epsilon = 0.015$; the former corresponds to a Maxwell material with two relaxation times. Increasing ϵ to 0.10 causes a prediction of slower drawdown. While this does bring the simulation closer to the data for $z \leq 0.4$ m, the overall effect is to make the fit poorer. Based on the available data, there is no reason to use any value other than $\epsilon = 0.015$.

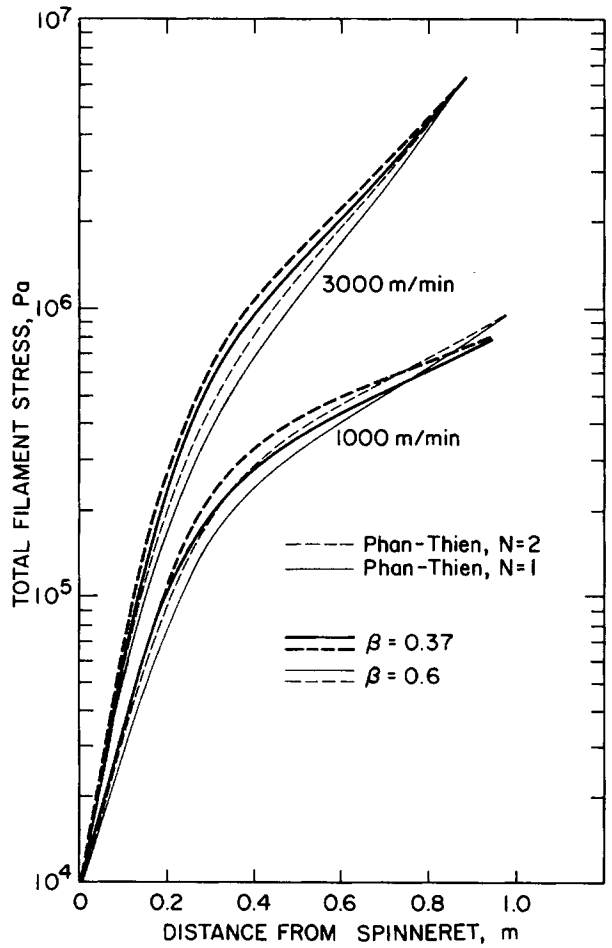

Fig. 8. Same as Fig. 3, but with $\beta = 0.37$ in Eq 3 for the drag coefficient.

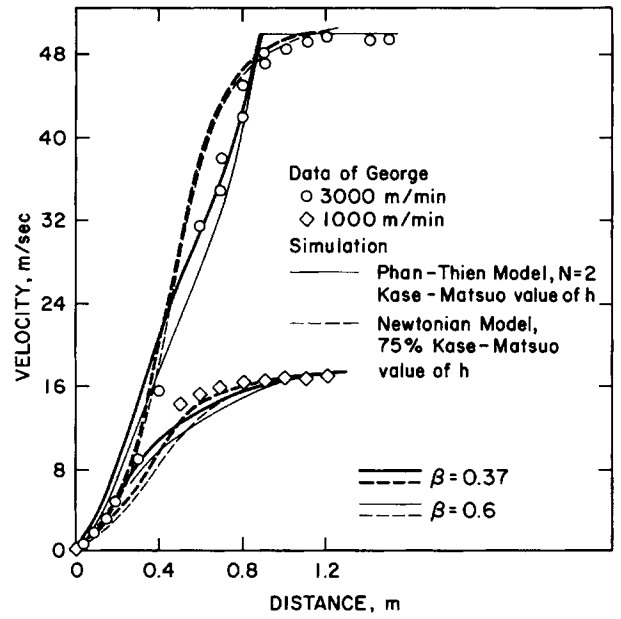

Fig. 9. Same as Fig. 7, but with $\beta = 0.37$ in Eq 3 for the drag coefficient.

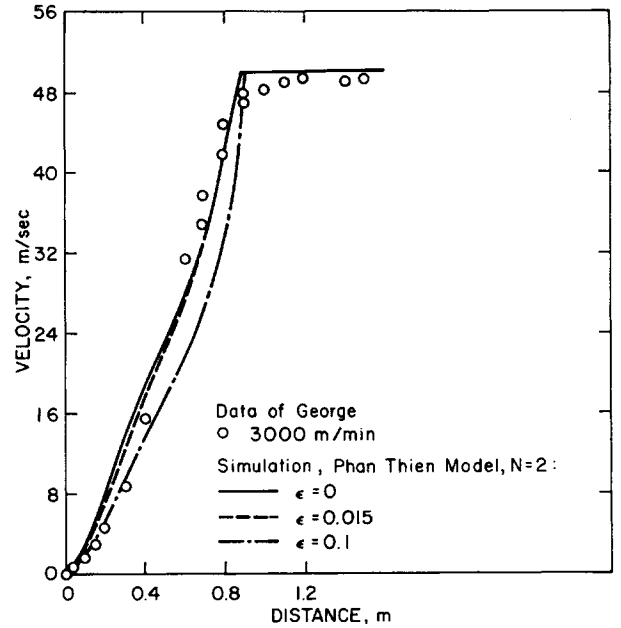

Fig. 10. Sensitivity of the simulation of the conditions in Table 1 to changes in the rheological parameter ϵ.

The dependence on the mean relaxation time is shown in *Figs. 11* and *12*. The calculations are done here for $N = 1$ in order to facilitate comparisons based on the relaxation time for PET measured by Gregory (25). It is evident from the velocity profile in *Fig. 11* and the computed stress at solidification in *Fig. 12* that the results are insensitive to changes in the mean relaxation time of up to 50 percent for the spinning conditions simulated here. Similar results are obtained for the lower drag coefficient. For a small relaxation time the stress approaches that for a Newtonian fluid, but under

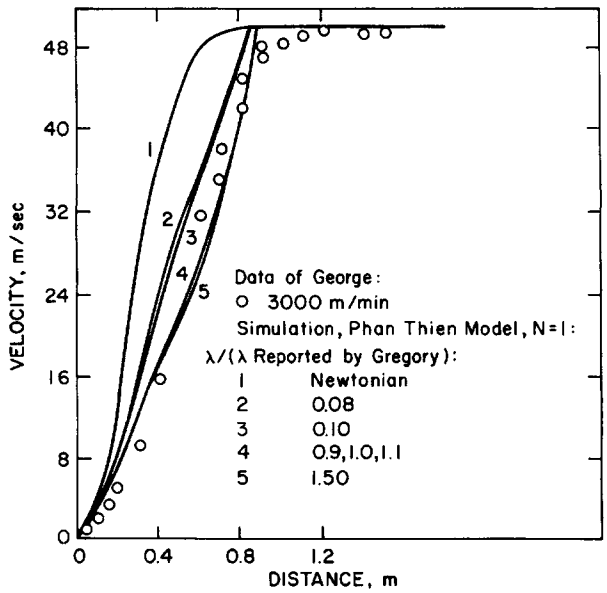

Fig. 11. Sensitivity of the simulation of the conditions in Table 1 to changes in the magnitude of the relaxation time.

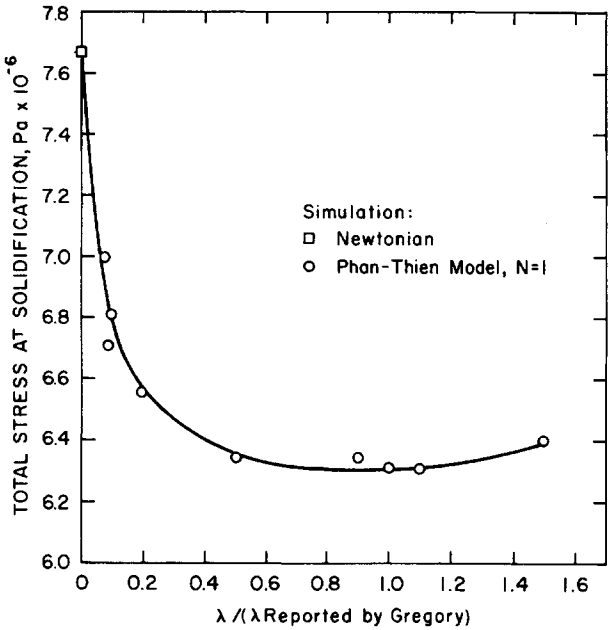

Fig. 12. Sensitivity of the calculated stress at solidification for spinning conditions in Table 1 to changes in the magnitude of the relaxation time.

these spinning conditions the stress in the viscoelastic liquid is always less than in the corresponding Newtonian fluid.

COMPUTER EXPERIMENTS

The simulations of George's experiments do not indicate important qualitative differences between the various rheological models. This is in part because of the spinning conditions employed. We show here the results of some computer experiments under somewhat different conditions of spinning PET, where differences do become important. Spinning conditions are tabulated in *Table 2*. Following Kase and Matsuo (24), the solidification temperature is taken here to be 60°C.

Table 2. Spinning Conditions for Computer Experiments

Polymer I. V.	0.67
Extrusion temperature	280°C
Air temperature	35°C
Air velocity	0.3 m/s
Initial diameter	0.5 mm

Figures 13 and *14* show velocity and temperature profile development, respectively, for a ten-denier (3.2×10^{-5} meter diameter) filament, manufactured at a takeup speed of 1000 m/min. The calculations are shown for viscoelastic and Newtonian fluids, both with (*high speed*) and without (*low speed*) air drag, inertia, and gravity. The viscoelastic calculation at these conditions

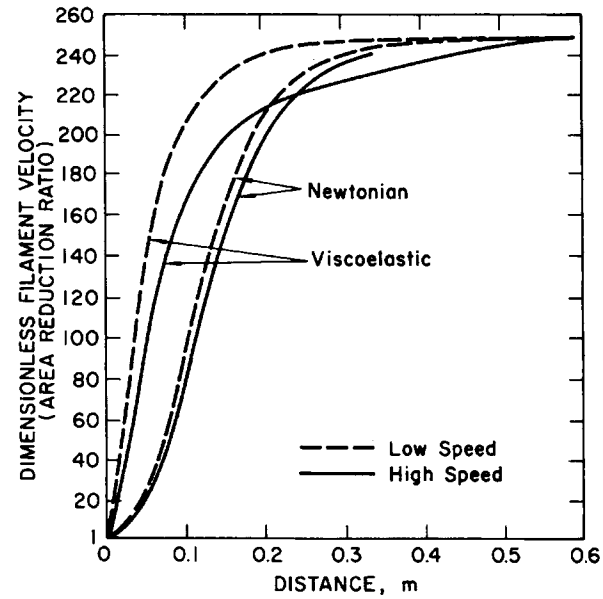

Fig. 13. Computed velocity profiles at 1000 m/min for spinning conditions in Table 2, using Newtonian and viscoelastic models, with and without inertia and air drag.

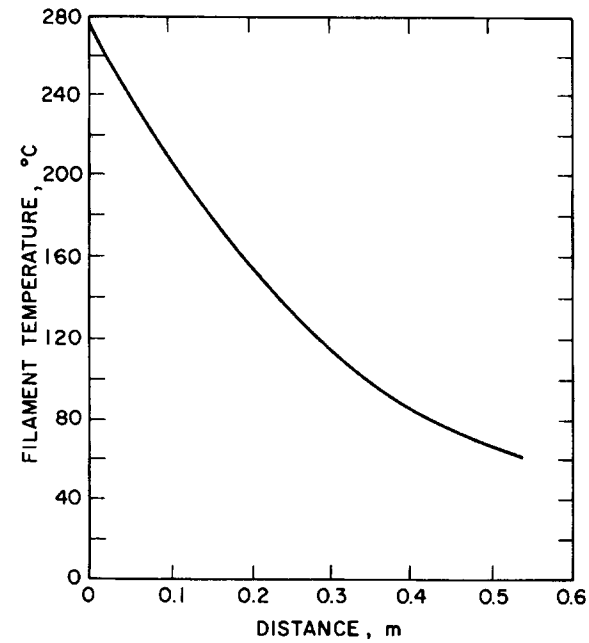

Fig. 14. Computed temperature profiles at 1000 m/min for spinning conditions in Table 2.

is the same for Maxwell and Phan-Thien models, using $N = 1$; at lower deniers, the results differ as noted subsequently. The filament temperature decrease is nearly exponential and independent of kinematics, consistent with the approximate solution of Fisher and Denn (13); the deviation from the single line shown in *Fig. 14* is no more than a few degrees for any of the four cases. The effect of inertia and air drag is to slow the rate of drawdown; gravity has no effect under these conditions. Neither inertia nor air drag individually causes deviation from the low speed profiles, but the effects are synergistic and together produce the results shown in *Fig. 13*.

Figure 13 points up two significant features of the simulation. First, there is a qualitative difference between the viscoelastic and Newtonian models, even for a polymer as inelastic as PET. Second, the effect of inertia and air drag is considerably greater in the viscoelastic model and operates in the opposite direction from the Newtonian fluid. Air drag increases the stress in a Newtonian liquid, while it *decreases* the stress in the viscoelastic liquid. This is evidently a consequence of the close coupling between the stress and the velocity history for a viscoelastic liquid. The slower draw retards the viscoelastic stress growth, resulting in a decrease in the computed stress. The stress development for this case is shown in *Fig. 15*. This type of result is one of the most important outputs of the simulation, since stress development parallels structure development in the filament.

Calculated stress at solidification for typical low and high speed cases is plotted as a function of draw ratio with lines of constant takeup speed in *Fig. 16*. At low takeup speeds and low denier (large drawdown) there is a tendency for the Maxwell model to predict very high stresses, with unbounded stresses at a critical draw ratio; this is the familiar behavior for low speed spinning (11).

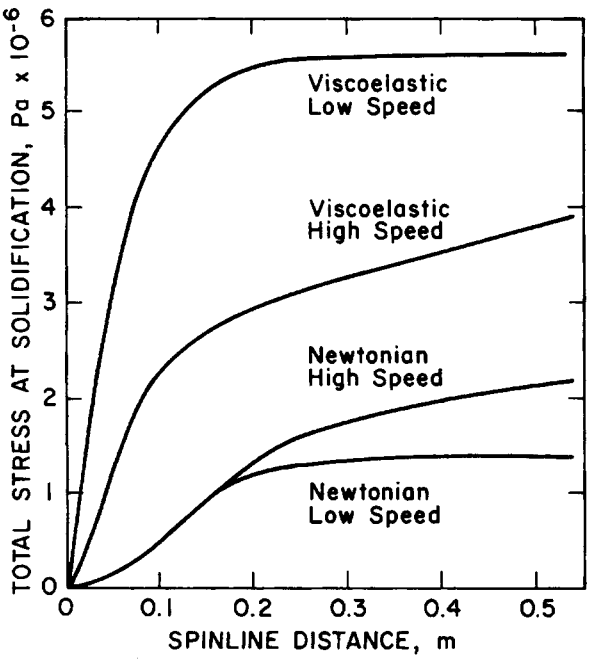

Fig. 15. Computed stress development at 1000 m/min for spinning conditions in Table 2.

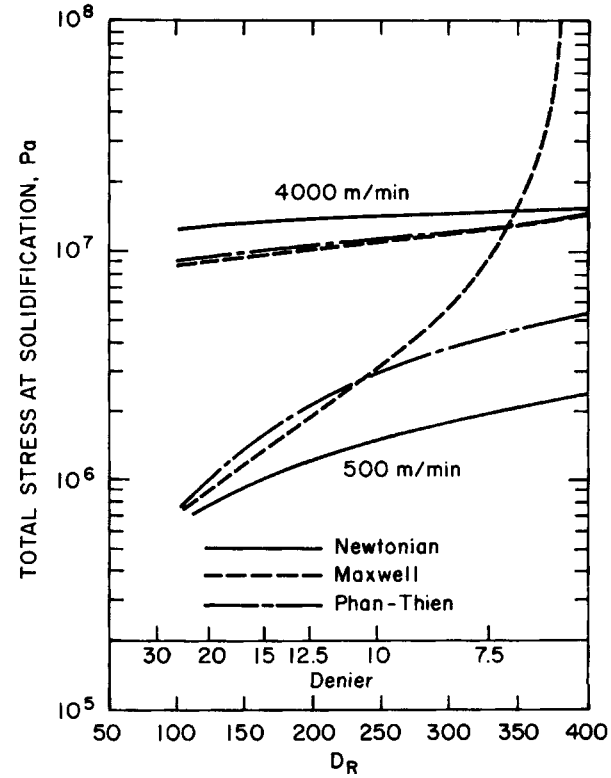

Fig. 16. Computed stress at solidification at 500 and 4000 m/min as a function of draw ratio for spinning conditions in Table 2.

At high takeup speeds, on the other hand, the Maxwell model indicates that stress growth is sufficiently retarded by inertia and air drag that stresses are always bounded and, indeed, are slightly lower than the stresses computed by the Newtonian model. (The absence of unbounded stresses when inertia is important might be expected from Petrie's analysis (2,11) of the effect of inertia on isothermal spinning.)

This curious interaction between high speed effects and viscoelasticity leads to some seemingly paradoxical behavior. Consider the manufacture of a 7.5 denier filament with the 0.5 mm initial diameter as an example. The Maxwell model predicts that the process could be carried out at speeds above about 3000 m/min and below about 500 m/min, but that stresses in the intermediate range would be excessive. Thus, by lowering throughput and takeup speed, conditions would be reached where the takeup stress would increase upon further reduction. Calculation of the stresses in the intermediate region is accomplished by the more realistic Phan-Thien rheological model, which gives results comparable to the Maxwell liquid at high speeds, and at low speeds with small drawdown ratios, but remains bounded. The Phan-Thien equation always leads to a takeup stress that increases monotonically with takeup speed at a given throughput; this is consistent with the known birefringence-takeup speed behavior in spinning practice, and serves as a consistency check on the rheological model. This calculation demonstrates the necessity of maintaining a nonzero value of ϵ in the simulation, and of obtaining a good estimate of this parameter for PET.

The effect of using one versus two relaxation times in the viscoelastic models is shown in *Fig. 17*. The use of two relaxation times in the Maxwell model causes a more rapid stress development, and the stress becomes unbounded at a lower critical draw ratio. On the other hand, the stresses calculated by the Phan-Thien model are only slightly affected by the use of two relaxation times.

STRESS-INDUCED CRYSTALLIZATION

Polyester filaments at takeup speed of less than 4000 m/min solidify as a noncrystalline material. Filaments drawn at 6000 m/min solidify with 20 to 45 percent crystalline regions (26-28). This transition takes place over a narrow range of spinning speeds. The semicrystalline polymer has physical properties that differ from the usual amorphous physical properties of the as-spun material. Theories of stress induced crystallization have been developed (1). Such theories have been coupled with hydrodynamic analyses of the spinning process only in qualitative terms, however, and a complete mechanical theory that includes crystallization has not yet been developed. We can hypothesize that the major effect of stress-induced crystallization is to introduce a load bearing crystal phase at a temperature greater than the glass transition, and hence to raise the effective solidification temperature. *Figure 18* shows the stress growth at 4000 m/min for a 10 denier filament at various solidification temperatures; the stress at the solidification point is only a weak function of solidification temperature, but the change should be measurable. *Figure 19* shows the dependence of stress at solidification with changes in solidification temperature; the effect at low

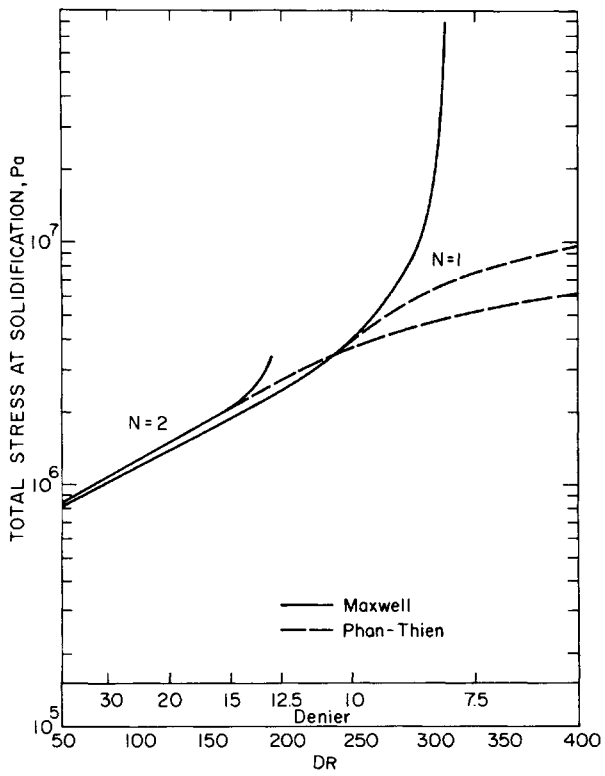

Fig. 17. Computed stress at solidification at 1000 m/min as a function of draw ratio for spinning conditions in Table 2.

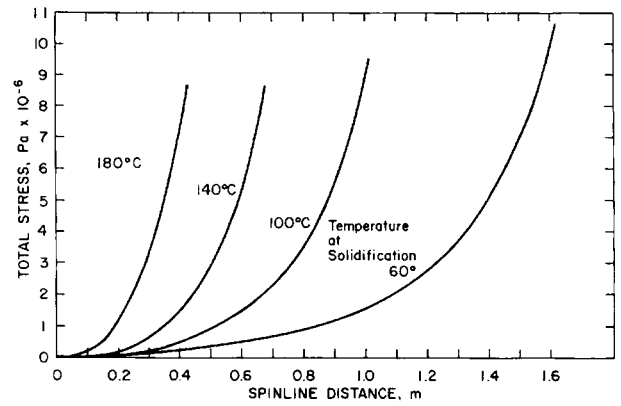

Fig. 18. Stress development at 4000 m/min for varying solidification temperatures, spinning conditions in Table 2.

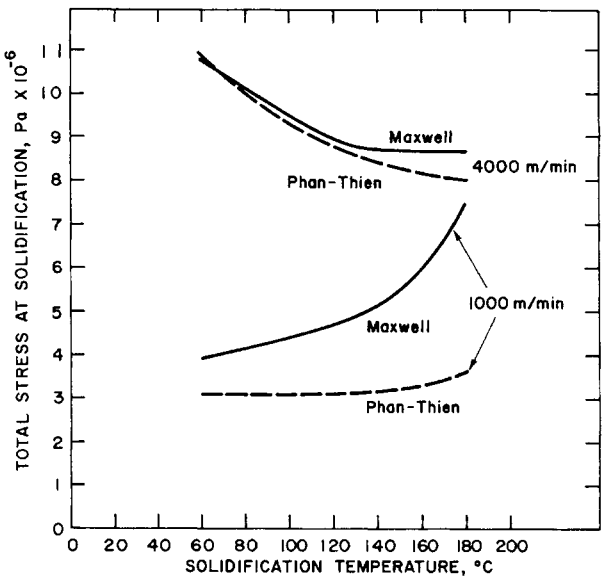

Fig. 19. Stress at solidification as a function of solidification temperature at 1000 and 4000 m/min, spinning conditions in Table 2.

speeds is opposite to that at high speeds. This behavior is demonstrated by both Phan-Thien and Maxwell fluid models. The calculation is relevant only at speeds above 4000 m/min, however.

This simple approach will not suffice for a crystalline polymer. Nadkarni and Shultz (29) show considerable diameter attenuation during crystallization in a spinning study on high-density polyethylene, for example, and Nadella, *et al.* (30) show crystallization occurring over a finite spin line length for isotactic polypropylene.

CONCLUSION

The simulation demonstrates that viscoelastic effects can be quite important in stress (and hence structure) development under some spinning conditions. The computer experiments with PET suggest that viscoelasticity is most important at low and intermediate spinning speeds; the retarding effect of high speed phenomena on stress growth results in stresses that are comparable to, but lower than, those in a Newtonian fluid with the viscosity of PET. The stress saturation embodied in the parameter ϵ in the Phan-Thien constitutive equation

plays no role under the conditions of the experiments simulated here, but the computer experiments under other spinning conditions show the stress saturation effect to be a potentially important one.

The interactive simulation program provides a tool for exploring the importance of uncertainties in stress and transport relations on the system response. The PET simulations demonstrate, for example, that small variations in the heat transfer coefficient correlation can result in large changes in the predicted drawdown, and that the absence of viscoelasticity in the spinning model can be compensated for by use of a smaller heat transfer coefficient.

ACKNOWLEDGMENT

This work was supported in part by the National Science Foundation under Grant ENG 76-15880. We appreciate the helpful comments of Dr. H. H. George, Prof. J. R. A. Pearson, and Dr. C. J. S. Petrie. A preliminary version of some of the results was presented at the AIChE 71st Annual Meeting, Miami, November, 1978. Some manuscript preparation was done while M. M. Denn was a Visiting Professor at the California Institute of Technology.

REFERENCES

1. A. Ziabicki, "Fundamentals of Fibre Formation," Wiley, N.Y. (1976).
2. C. J. S. Petrie, "Elongational Flows," Pitman, London (1979).
3. M. M. Denn, *Ann. Rev. Fluid Mech.*, **12**, 365 (1980).
4. S. Kase and T. Matsuo, *J. Polym. Sci.*, **A-3**, 2541 (1965).
5. L. R. Glicksman, *J. Basic Eng.*, **90**, 343 (1968).
6. I. Hamana, M. Matsui, and S. Kato, *Melliand Textilber*, **50**, 382, 499 (1969).
7. H. H. George, paper presented at Second Joint U.S.-Japan Societies of Rheology Meeting, Kona, Hawaii (April, 1979).
8. H. Yasuda, H. Ishihara, and H. Yanagawa, *Sen-i Gakkaishi*, **34**, T19 (1978).
9. H. Yasuda, H. Sugiyama, and H. Yanagawa, *Sen-i Gakkaishi*, **35**, T370 (1979).
10. M. Stehle and R. Brückner, *Glastechn. Ber.*, **52**, 82, 105 (1979).
11. M. M. Denn, C. J. S. Petrie, and P. Avenas, *AIChE J.*, **21**, 791 (1975).
12. R. J. Fisher and M. M. Denn, *AIChE J.*, **22**, 236 (1976).
13. R. J. Fisher and M. M. Denn, *AIChE J.*, **23**, 23 (1977).
14. J. L. White and Y. Ide, *J. Appl. Polym. Sci.*, **22**, 3057 (1978).
15. M. M. Denn and G. Marrucci, *J. Non-Newt. Fluid Mech.*, **2**, 159 (1977).
16. N. Phan-Thien, *J. Rheol.*, **22**, 259 (1978).
17. C. J. S. Petrie, *J. Non-Newt. Fluid Mech.*, **4**, 137 (1978).
18. M. Matsui and D. C. Bogue, *Polym. Eng. Sci.*, **16**, 735 (1976).
19. N. Phan-Thien and R. I. Tanner, *J. Non-Newtonian Fluid Mech.*, **2**, 353 (1977).
20. D. K. Gagon, M. Ch.E. Thesis, University of Delaware, Newark (1980).
21. M. A. Matovich and J. R. A. Pearson, *Ind. Eng. Chem. Fundam.*, **8**, 512 (1969).
22. R. J. Fisher, M. M. Denn, and R. I. Tanner, *Ind. Eng. Chem. Fundam.*, **19**, 195 (1980).
23. M. Matsui, *Trans. Soc. Rheol.*, **20**, 465 (1976).
24. S. Kase and T. Matsuo, *J. Appl. Polym. Sci.*, **11**, 251 (1967).
25. D. R. Gregory, *Trans. Soc. Rheol.*, **17**, 191 (1973).
26. J. Shimizu, K. Toriumi, and K. Tamai, *Sen-i Gakkaishi*, **33**, T208 (1977).
27. H. M. Heuvel and R. Huisman, *J. Appl. Polym. Sci.*, **22**, 2229 (1978).
28. H. R. E. Frankfort and B. H. Knox, U. S. Patent No. 4, 134, 882 (1979).
29. V. M. Nadkarni and J. M. Schultz, *J. Polym. Sci., Polym. Phys. Ed.*, **15**, 2151 (1977).
30. H. P. Nadella, H. M. Heuson, J. E. Spruiell, and J. L. White, *J. Appl. Polym. Sci.*, **21**, 3003 (1977).